NANO LETTERS

LETTER

pubs.acs.org/NanoLett

# Light Interactions with Gold Nanorods and Cells: Implications for Photothermal Nanotherapeutics

Constantin Ungureanu,[*,†] Rene Kroes,[†] Wilma Petersen,[†] Tom A. M. Groothuis,[‡] Felicia Ungureanu,[‡] Hans Janssen,[§] Fijs W. B. van Leeuwen,[∥] Rob P. H. Kooyman,[‡] Srirang Manohar,[*,†] and Ton G. van Leeuwen[†,⊥]

[†]Biomedical Photonic Imaging Group, MIRA Institute for Biomedical Technology and Technical Medicine, Faculty of Science and Technology, University of Twente, P.O. Box 217, 7500 AE Enschede, The Netherlands

[‡]Nanobiophysics Group, Faculty of Science and Technology, University of Twente, P.O. Box 217, 7500 AE Enschede, The Netherlands

[§]Division of Cell Biology, The Netherlands Cancer Institute, 1066 CX Amsterdam, The Netherlands

[∥]Division of Diagnostic Oncology, The Netherlands Cancer Institute, 1066 CX Amsterdam, The Netherlands

[⊥]Biomedical Engineering and Physics, Academic Medical Center, University of Amsterdam, P.O. Box 2270, 1100 DE Amsterdam, The Netherlands

Supporting Information

**ABSTRACT:** Gold nanorods (AuNR) can be tailored to possess an intense and narrow longitudinal plasmon (LP) absorption peak in the far-red to near-infrared wavelength region, where tissue is relatively transparent to light. This makes AuNRs excellent candidates as contrast agents for photoacoustic imaging, and as photothermal therapeutic agents. The favorable optical properties of AuNR which depend on the physical parameters of shape, size and plasmonic coupling effects, are required to be stable during use. We investigate the changes that are likely to occur in these physical parameters in the setting of photothermal therapeutics, and the influence that these changes have on the optical properties and the capacity to achieve target cell death. To this end we study 3 sets of interactions: pulsed light with AuNR, AuNR with cells, and pulsed light with cells incubated with AuNR. In the first situation we ascertain the threshold value of fluence required for photothermal melting or reshaping of AuNR to shorter AuNR or nanospheres, which results in drastic changes in optical properties. In the second situation when cells are exposed to antibody-conjugated AuNR, we observe using transmission electron microscopy (TEM) that the particles are closely packed and clustered inside vesicles in the cells. Using dark-field microscopy we show that plasmonic interactions between AuNRs in this situation causes blue-shifting of the LP absorption peak. As a consequence, no direct lethal damage to cells can be inflicted by laser irradiation at the LP peak. On the other hand, using irradiation at the transverse peak (TP) wavelength in the green, at comparative fluences, extensive cell death can be achieved. We attribute this behavior on the one hand to the photoreshaping of AuNR into spheres and on the other hand to clustering of AuNR inside cells. Both effects create sufficiently high optical absorption at 532 nm, which otherwise would have been present at the LP peak. We discuss implications of these finding on the application of these particles in biomedicine.

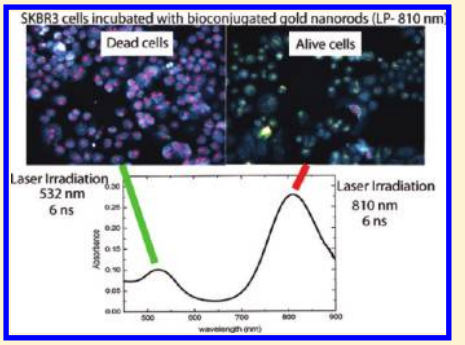


**KEYWORDS:** Gold nanorods, photoacoustic imaging, photothermal therapy, dark-field imaging

The phenomenon of surface plasmon resonance refers to the exciting of coherent oscillations of free electrons at the surfaces of silver/gold nanoparticles by light of a specific frequency.[1,2] Consequently light of the appropriate wavelength interacts strongly with the silver/gold nanoparticles leading to intense absorption and scattering peaks called plasmon peaks in the optical spectra.

Gold nanospheres (AuNS) have a single plasmon resonant peak around 520 nm. Gold nanorods (AuNR) due to their asymmetry permit two plasmons to be excited along the axes of the particle, leading to the longitudinal plasmon (LP) peak, and the transverse plasmon (TP) peak in the spectra. The latter remains at around 520 nm while the LP peak position can be tuned by changing the aspect ratio of the particle using popular wet-chemistry synthesis methods[3] to provide particles that have strong absorbing peaks between 650 and 950 nm.[4]

AuNRs are considered for various light-based imaging and therapeutic applications because light penetrates deeply into tissue (10 mm+) in the range of 700−1100 nm, as it undergoes less absorption and scattering by tissue components.[5] One of the most promising of these imaging techniques is photoacoustics, which relies on absorption of nanosecond (ns) pulsed light to

**Received:** November 4, 2010
**Revised:** March 29, 2011
**Published:** April 14, 2011

generate ultrasound due to rapid heating and thermoelastic expansion. Photoacoustic imaging has been used to detect pathologies such as cancer using their intrinsic absorption contrast with respect to normal tissue.[6−8] As early as 2001, a potential synergy between AuNRs with their strong absorptions, and photoacoustic imaging was recognized,[9] with the particles envisaged as contrast agents.[10−13] The AuNRs could be made to accumulate at the disease site of interest, and then a more sensitive and specific detection/diagnosis of the pathology could be achieved.

It is also known that by delivering continuous wave (CW) light of optimal exposures the absorption by the particles can cause sufficient heating and temperature rise to kill cells, opening up therapeutic applications.[10,14−21] In addition to the CW regime, the use of pulsed radiation has been shown to cause bubble formation and subsequent cavitation of media surrounding the NRs[22,23] causing cell death. In the spirit of molecular theranostics, one could use a nanosecond pulsed laser to perform conventional AuNR mediated photoacoustic detection of the pathology and, subsequently, use higher energies from the same ns laser to achieve photothermal therapy of the disease.[24,25]

While the effects of irradiation with subnanosecond regime of gold nanorods have been extensively studied,[10,22,26−30] there are only a few studies reported on the pulse duration range (5−10 ns) in use for photoacoustics. Of the few reports, Takahashi et al.[31] showed that cells could be killed with precise localization using AuNR and focused NIR pulses at fluences around 900 mJcm$^{-2}$. They suggested that cell-damage occurs in the first pulse(s) of illumination at the LP peak, since AuNR can be drastically reshaped at fluences lower than those used for the killing. The same authors showed[32] that the reshaping of AuNRs with fluences of 175 mJ cm$^{-2}$ (pulse duration 5−7 ns, repetition rate 10 Hz) could be used as a safety mechanism to prevent further cell death, since absorption by the new particles in the NIR wavelengths was nominally zero.

Thus, there is a caveat when using short light pulses to illuminate AuNR: it has been shown early on[33−38] that if short (ns, fs, ps) high energy pulses are used intense AuNR heating can induce melting and fragmentation of the particles. The originally rod-shaped nanoparticle is thus converted into a nanosphere (NS) or a shorter aspect ratio (AR) AuNR. This morphology change implies that the red-shifted LP peak, which is the primary reason for interest in AuNRs is lost, and the spectrum shows only the solitary plasmon peak in the green, characteristic of AuNSs. The implications of this reshaping for imaging and therapy are evident: the high absorptions of the particles at the near-infrared (NIR) wavelengths are drastically reduced, so that they cannot perform the contrast enhancing or photothermal therapeutic effect at the original wavelength.

For maximizing the efficacy of these nanoparticles for biomedical applications, the particles need to retain their strong NIR optical absorptions and thus their shape during the imaging or therapeutic procedure. This would mean that particles should be excited with fluences lower than the reshaping threshold, a value which has been quoted as being between 20 and 43 mJ cm$^{-2}$ by Didychuk et al.[24] and between 150 and 200 mJ cm$^{-2}$ by Takahashi et al.[31,32] The group of Pai-Chi Li[39,40] and Emelianov[41] reported that reshaping occurs under 20 mJ cm$^{-2}$ for NIR irradiation with pulses (5−7 ns).

Thus, there is as yet no consensus in range of threshold fluences required to initiate AuNR photothermal deformation.

In addition to this hindrance in the use of the AuNR, another issue is that particles internalized by cells can approach close to each other or could form clusters,[42] which affect the optical properties of the particles, due to plasmon coupling effects.[43,44] The clusters and aggregates of particles when illuminated with subnanosecond light pulses at 532 nm and NIR have been shown to cause cell death.[22,26,45−47] However, we could not find literature which describes the same effects when lasers with pulse duration of several nanoseconds and NIR irradiation on cells incubated with bionconjugated gold nanorods and this aspect was analyzed also in this work.

To summarize, there is a paucity of studies using light excitation in the photoacoustic pulse duration regime to achieve cell-death mediated by AuNR, in the context of the perils faced by AuNRs and their optical properties. In this work, we revisit the scenario of ns pulsed light interaction with AuNR, as also the scenario of particle interaction with cells, in the setting of photothermal therapeutic applications and provide new insights. We first ascertain the reshaping threshold fluence of AuNR by illuminating the particles in well-plates with increasing energies and analyzing their optical spectra. AuNR are then conjugated with anti-HER2 (HER81) mAbs using a covalent binding involving a PEG-linker. The mAb-AuNR are incubated with human breast carcinoma cell line (SKBR3) cells for different time-periods and imaged using dark-field microscopy with and without laser irradiation. The irradiation is chosen to be clearly above or below the obtained reshaping threshold using both NIR and green light. Cell viability is monitored with fluorescence microscopy using membrane permeability to propidium iodide (PI) as the indicator of cell death. Cellular uptake of mAb-AuNR particles in SKBR3 cells is also investigated using transmission electron microscopy (TEM). The most important finding is that no direct lethal damage to cells can be inflicted by laser irradiation at the LP peak. On the other hand, using irradiation at the transverse peak (TP) wavelength in the green, at comparative fluences, extensive cell death can be achieved. We discuss these results and their implications in biomedical applications.

**Materials and Methods.** *Synthesis and Bioconjugation of Gold Nanorods.* AuNRs with a longitudinal plasmon peaks (LP) at 640, 713, and 810 nm were synthesized using a seed-mediated, surfactant and silver assisted growth protocol.[4] In this protocol, based on the work of Nikoobakht and El-Sayed,[3] elongated gold nanoparticles are grown from CTAB (cetyltrimethylammonium bromide) capped gold nanospheres in the presence of CTAB, $AgNO_3$ (silver nitrate), and $HAuCl_4$ (chloroauric acid).

Details are available in Rayavarapu et al.;[4] we mention only that in order to obtain $AuNR_{640}$, $AuNR_{713}$, or $AuNR_{810}$ we require respectively the following ratios of gold to silver in the growth solutions: 1:0.06, 1:0.12, and 1:0.24, respectively.

The absorbance (optical extinction, $\mu_{ext}$) spectra of the AuNR were measured using a Shimadzu PC3101 UV−vis−NIR spectrophotometer. High resolution scanning electron microscopy (HR-SEM) images of the gold nanorods were acquired using a Zeiss−1550 HR-SEM. The concentration of the synthesized particles ($N$) was determined as $N = \mu_{ext}/\sigma_{ext}$, where $\mu_{ext}$ is the extinction coefficient and $\sigma_{ext}$ is the extinction cross-section of the particles calculated as in ref 48.

A scheme of the bioconjugation protocol is shown in Figure 1. The mAb was covalently bound to an OPSS (pyridyl dithio-PEG succinimidylpropionate) linker. This was attached to the AuNR surface via the disulfide group. Three 2 mL microtubes of AuNR were centrifuged at 7000$g$

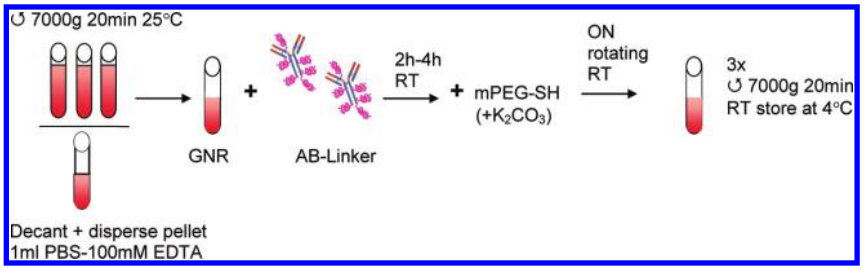


**Figure 1.** Scheme of procedure for the bioconjugation of AuNR with HER81 mAb.

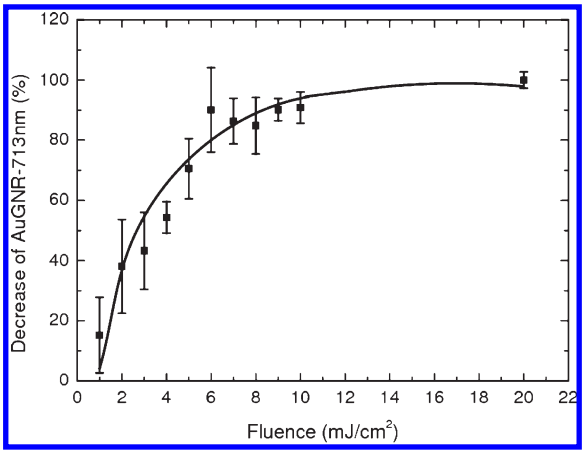


**Figure 2.** Decrease in amplitude of the LP of $AuNR_{713}$ as a function of incident laser fluence at 713 nm. The threshold fluence ($F_{th}$) at which 50% of the NR are reshaped is 3.5 $mJcm^{-2}$ for 1 min exposure at 10 Hz. The line is drawn to guide the eye.

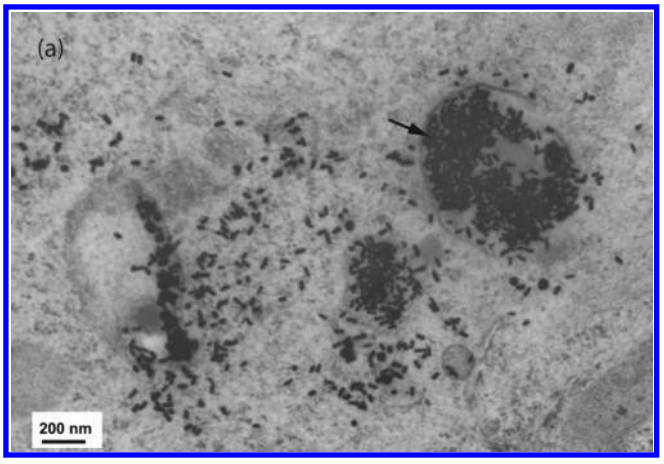


**Figure 3.** Transmission electron micrograph of a SKBR3 cell section incubated with mAb-$AuNR_{810}$ nm for 24 h. AuNRs can be seen as single particles and clusters (marked with arrow, right side of the image).

for 20 min at 25 °C. The pellets were added together and dispersed in 1 mL of PBS (phosphate buffered saline) with a final concentration of 100 mM EDTA and mixed gently. Next 5 $\mu$g of HER81-OPSS was added while vortexing and allowed to stand for 2−4 h at RT.

After incubation, 100 $\mu$L of 2 mM $K_2CO_3$ (potassium carbonate) and 12 $\mu$L of 5 mM mPEG-SH were added, and the sample was rotated overnight at room temperature (RT). Further, the sample was centrifuged 3× at 7000*g*/20 min and the supernatant was discarded. The pellet was dissolved in 1 X PBS and stored at 4 °C.

*Cell culture.* SKBR3 cells (HER2 positive mammary adenocarcinoma) were cultured at 37 °C and 5% $CO_2$ in RPMI 1640 medium (Invitrogen) supplemented with glutamine and 10% FBS (fetal bovine serum) with antibiotics. For experiments cells were cultured on 12 mm glass coverslips.

*TEM Imaging of mAb-AuNR Exposed Cells.* Due to attenuation of the electron beam by the AuNRs, their interaction with cells can be accurately visualized at the nm-scale using transmission electron microscopy (TEM). SKBR3 cells were exposed to the mAb-$AuNR_{810}$ for 24 h. The concentrations used were 30 pM ($18 \times 10^9$ NR/ml). Exposed cells were fixed in Karnovsky fixative. Postfixation was done with 1% osmium tetroxide in 0.1 M cacodylate buffer. After washing, the pellets were dehydrated via ethanol dehydration series. Finally the cells were embedded in a mixture of DDSA/NMA/Embed-812 (EMS, Hatfield, USA), sectioned and stained with Ultrastain-1 (Leica, Vienna, Austria) followed by lead oxide and analyzed with a CM10 electron microscope (FEI, Eindhoven, The Netherlands).

*Laser Irradiation Protocol of SKBR3 Cells Incubated with mAb-AuNR.* After two days of cell culture, media was removed from the cells and replaced with 100 $\mu$L of mAb-$AuNR_{810}$ (or mAb-$AuNR_{640}$) at a concentration of $18 \times 10^9$ NR/mL for a period of 24 h. The AuNRs were premixed with fresh media. After incubation the cells were rinsed with PBS, and fresh medium was added prior to laser irradiation. The irradiation of the SKBR3 cells incubated with mAb-$AuNR_{810}$ used the Nd:YAG coupled with OPO (pulse duration 6 ns) at the following wavelengths:

- 810 nm: fluence per pulse of 4.3, 21, and 62 mJ $cm^{-2}$
- 532 nm: fluence per pulse of 11 and 61 mJ $cm^{-2}$

In the case of SKBR3 cells incubated with mAb-$AuNR_{640}$ the following wavelength was used for irradiation:

- 700 nm: fluence per pulse of 20 and 100 mJ $cm^{-2}$

Following irradiation, the cells were incubated with propidium iodide (PI) for 1 h to stain for cellular death. The cells were then washed with fresh medium and visualized in dark-field microscopy. The dark-field images were acquired with an inverted microscope (Olympus), dark field objective: MPLAN (20×/2×) (Olympus), camera Carl Zeiss HRc (14 bits).

**Results and Discussion.** *Threshold Fluence for Reshaping CTAB-AuNRs.* In order to investigate the reshaping process of AuNRs in solution, volumes of 200 $\mu$L of CTAB-$AuNR_{713}$ in a multiwell plate were illuminated with different radiant exposures ranging from 1 to 20 mJ $cm^{-2}$ per pulse at the LP peak. Experimental detail can be found in the Supporting Information.

The conversion of AuNR to gold nanospheres (AuNS) or shorter aspect ratio particles was quantified by calculating the


dx.doi.org/10.1021/nl103884b |*Nano Lett.* 2011, 11, 1887–1894

relative decrease in the amplitude of the LP peak. In an ensemble collection of $10^{11}$ particles in a 200 $\mu$L volume, the macroscopic absorbance spectrum is the collective effect of the individual responses. Reshaping of the particles is probabilistic and a statistical measure for threshold fluence ($F_{th}$) can be defined by the value at which 50% of the AuNR have undergone reshaping, where the LP peak has fallen to 50% of its initial value. Figure 2 shows the % conversion as a function of the incident laser fluence.

From Figure 2 we see that from 6 mJ cm$^{-2}$ onward more than 95% of the AuNR are reshaped for 1 min exposure at 10 Hz. The threshold fluence ($F_{th}$) at which 50% of the NR are reshaped can be identified as 3.5 mJ cm$^{-2}$ for 1 min exposure at 10 Hz. The values of threshold reshaping fluence for AuNRs with LP peaks at 713 and 810 nm were for all practical purposes similar. At 640 nm, the threshold was not measured as no laser emitting at 640 nm 6 ns pulse widths was available. We make the assumption that for 600 pulses exposure, the threshold for $AuNR_{640}$ is not different from that for $AuNR_{713}$ and $AuNR_{810}$.

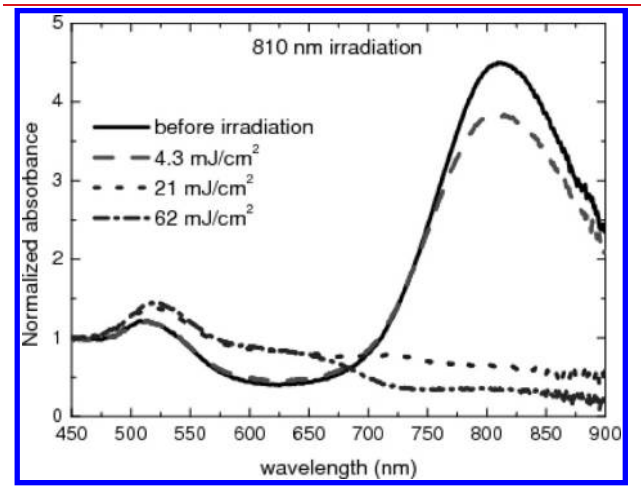


**Figure 4.** Absorbance spectra of $AuNR_{810}$ pre- and postirradiation using 4.3, 21, and 62 mJ cm$^{-2}$ at the LP peak wavelength. The absorbance peak at 810 nm reduces with increasing laser fluences until complete disappearance for the highest fluence. Irradiation was for 1 min long at 10 Hz.

*Electron Microscopic Evidence of AuNR Clustering in Cellular Uptake.* Figure 3 is the TEM image of an embedded cell section of SKBR3 cells incubated for 24 h with mAb-$AuNR_{810}$. AuNRs are seen present individually or closely packed in vesicles. When mAb-AuNRs interact with target cells, they can be taken up by the cells. The particles will be internalized in vacuoles. This confinement of the particles will bring several AuNR in close proximity which are likely to cause plasmon coupling effects[49,50] which will affect the optical properties.

*Laser Irradiation at 810 nm of SKBR3 Cells Incubated with mAb-$AuNR_{810}$.* As seen above AuNRs can be reshaped at a fluence as low as 3.5 mJ cm$^{-2}$, which is well below the maximal permissible threshold (MPE) which is 30 mJ cm$^{-2}$ for 800 nm or 600 pulses.[13] In order to ascertain the optical properties post-irradiation for the fluences that we intended to use for the cell-$AuNR_{810}$ experiments, we performed experiments with the $AuNR_{810}$ in cuvettes using fluences of 4.3, 21, or 62 mJ cm$^{-2}$. Only the latter fluence is higher than the MPE.

Morphological analysis of the particles after irradiation (laser fluences 17 mJ cm$^{-2}$) reveal that they maintain their volume with reduction in aspect ratio (particle melt). Using this information we can further explain the appearance of cells incubated with mAb-AuNR in dark-field microscopy. (See the Supporting Information, Figure 3.)

The optical absorbance spectra of the particles pre- and post-irradiation are shown in Figure 4. The original LP peak amplitude shows a small decrease for irradiation with 4.3 mJ cm$^{-2}$ with complete disappearance at 21 and 62 mJ cm$^{-2}$. The spectra were normalized at 450 nm because at this wavelength the effects of reshaping on spectra are negligible. The mAb-AuNR have slightly higher resistance to reshaping than CTAB-AuNR due to the presence of amphiphilic molecules bound to the NR surface[51] which spontaneously form molecular assemblies. Further, the mAb-AuNRs have water molecules held within the PEG-linker chains; this layer will possess a higher thermal diffusivity leading to faster heat losses and less efficient heat buildup in contrast to a CTAB-layer.

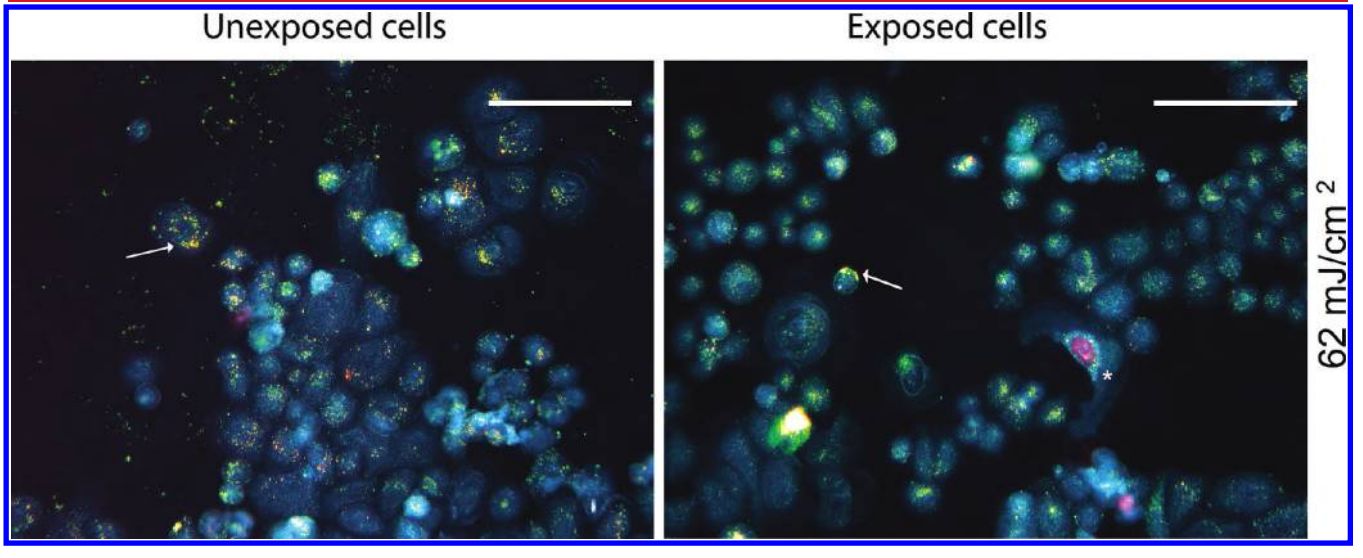


**Figure 5.** Dark-field light scattering microscopic images (scale bar 50 $\mu$m) of SKBR3 cells incubated with mAb-$AuNR_{810}$ for 24 h, (left) nonirradiated and (right) irradiated with 810 nm for 1 min at 10 Hz and using 62 mJ cm$^{-2}$ per pulse. White arrows represent mAb-$AuNR_{810}$ nanoparticle clusters and white asterisk cells positive for PI.


dx.doi.org/10.1021/nl103884b |*Nano Lett.* 2011, 11, 1887–1894

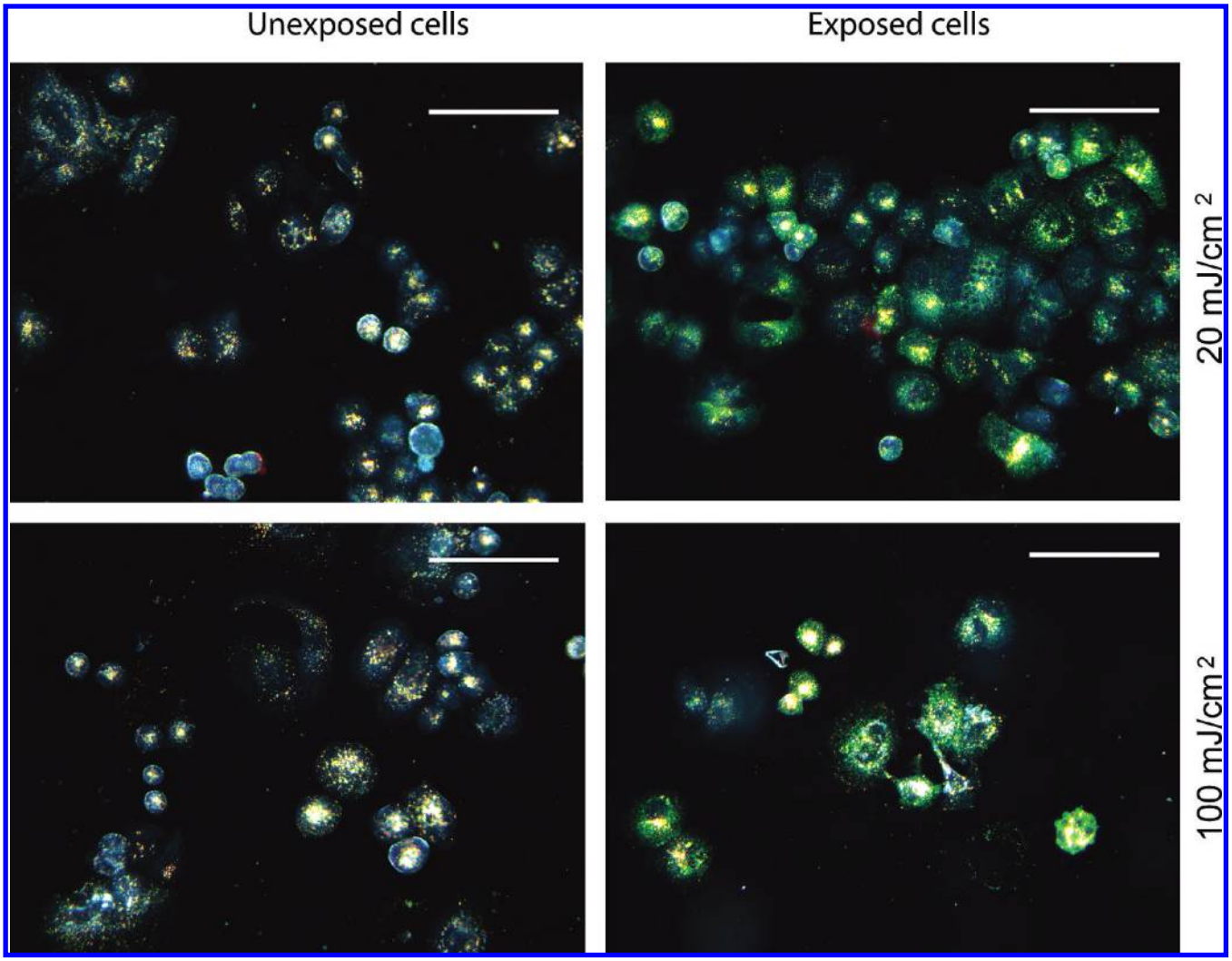


**Figure 6.** Dark field microscopic images (scale bar 50 $\mu$m) of SKBR3 cells incubated with mAb-AuNR$_{640}$ for 24 h. Left column nonirradiated cells and right column irradiated cells with an applied fluence of 20 mJcm$^{-2}$ for the first row and 100 mJ cm$^{-2}$ for the second row. Wavelength of light was 700 nm and exposure was for 1 min at 10 Hz. No significant PI uptake is seen indicating that the cells are viable. Nonirradiated cells show scattering in the orange and irradiated cells scatter predominantly in the green part of the spectrum.

Next we determined the effect of illumination at 810 nm on the cells incubated for 24 h with mAb-AuNR$_{810}$. Figure 5 shows dark-field microscopic light-scattering images of nonirradiated, and irradiated cells. The high-intensity scattered light corresponds to positions where the AuNRs are present. Scattering from inside the cells indicates high cellular uptake of the particles. In the non-irradiated case (Figure 5a), the light-scattering colors are green and orange-red. We attribute the green to the transverse plasmon (TP) of the particles; scattering at the LP wavelength cannot be visualized due to the sensitivity cutoff of the detector at around 700 nm. The orange-red (arrows in Figure 5) is likely to be due to the clustering of AuNR in vesicles within the cell,[42] which causes a shift of the LP peak from 810 nm of the individual particles. The postirradiation (Figure 5b) light-scattering colors are largely green, but yellow to orange-red are also observed. We believe that the relative increase in green (and yellow) is due to the reshaping of the AuNR to nanospheres (and shorter AR rods). At the fluence of 61 mJ cm$^{-2}$, all of the particles are expected to be reshaped.

The light-scattering color changes exhibited by the particles following reshaping can be better appreciated by repeating the above experiments with mAb-AuNR$_{640}$, whose LP peaks fall within instrumentation sensitivity of the dark-field setup. Irradiation was performed at 700 nm with fluences of 20 and 100 mJcm$^{-2}$. The dark-field light scattering images for non-irradiated and irradiated cells (Figure 6) show striking differences in color.

The nonirradiated and intact particles show light scattering in the orange region, whereas the irradiated AuNRs are predominantly green in color. The green appearance shows that reshaping of the AuNRs into nanospheres has occurred. As in the previous case, there is no PI uptake indicating that the cells are viable. Thus, irradiation at the LP peaks of AuNRs dispersions in which the cells were incubated did not result in lethal damage to the cells, although the AuNRs were reshaped by the moderately intense laser pulses. The green appear more intense in this case (cells incubated with mAb-AuNR$_{640}$) because these particles have effective radiuses higher than AuNR$_{810}$,[48] which in turns provide a higher scattering cross-section.

No significant cell death, either following incubation with the mAb-AuNR or after high fluence irradiation at the LP is


dx.doi.org/10.1021/nl103884b |*Nano Lett.* 2011, 11, 1887–1894

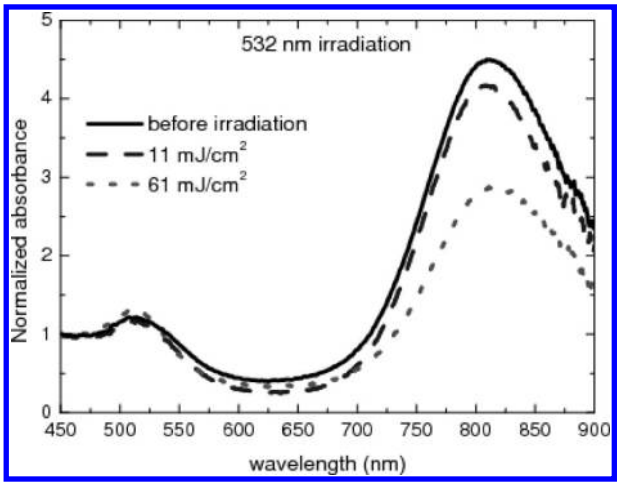


**Figure 7.** Absorbance spectra of $AuNR_{810}$ pre- and postirradiation by 600 pulses using 11, and 61 mJ $cm^{-2}$ fluences per pulse at 532 nm close to the TP peak wavelength. The absorbance peak at 810 nm reduces with the increasing laser fluences. the.

observed. According to Link et al,[52] Plech et al[53] the thermal reshaping of AuNR is a fast phenomenon, which occurs between 30 and 50 ps or at least under 100 ps. The deformation thus occurs well within the 6 ns duration of the heating laser pulse. During the reshaping time, the optical energy absorbed by the AuNR is used for the reorganization of the crystalline matrix along defects followed by diffusion, to form nanospheres and smaller AuNRs. Thus the rest of the energy after this period, until the end of the ns pulse will no longer be absorbed by the particle, due to its blue-shifted absorption peak. Consequently the heat diffusion and temperature rise in the adjacent cells is low, which spares them from damage, for the rest of the pulse and subsequent pulses. However recent experiments from Hleb et al[54] suggest that NRs do not melt within 500 ps and the LP peak is retained following a pulse. At this point we cannot corroborate or refute this, however our results can be explained by invoking refs 33, 52, and 55.

*Laser Irradiation at the TP Peak (532 nm) of SKBR3 Cells Incubated with mAb-$AuNR_{810}$.* To investigate if excitation at the TP peak could cause any effects on cells, we repeated the above experiments using ns pulses at 532 nm at 11 and 61 mJ $cm^{-2}$ per pulse (Figure 7). The former fluence is lower and the latter higher than the MPE at this wavelength (20 mJ $cm^{-2}$ for 600 pulses.)[13]

Irradiation of the particles in bulk at the TP wavelength for 1 min at 10 Hz repetition rate caused a slight reduction in the LP peak amplitude for 11 mJ $cm^{-2}$ and a 40% drop for 61 mJ $cm^{-2}$ pulses. The changes are not as dramatic as observed in Figure 4 due to the lower $C_{abs}$ and consequently lower heating of $AuNR_{810}$ at 532 nm when compared to 810 nm irradiation.

Figure 8 shows the dark-field microscopic light-scattering images of nonirradiated and irradiated SKBR3 cells incubated with mAb-$AuNR_{810}$ for 24 h. In the nonirradiated cases, the light-scattering colors are green and orange-red due to the same explanation for the colors in Figure 5: green is from the transverse plasmon (TP) of the AuNR and the orange-red due to clustering of AuNR in vesicles in the cells. After irradiation at 11 mJ $cm^{-2}$, no significant changes in the light-scattering spectra and no PI uptake is observed.

After irradiation with 61 mJ $cm^{-2}$, the most striking feature of the images is the PI uptake by the entire cell population: the cells are dying or dead. This is in contrast to the high cell viability observed under identical conditions but when the LP of the particles were excited with 62 mJ $cm^{-2}$. (Figure 5).

We surmise that the extensive cell-death after irradiation with 532 nm laser pulses which is not observed with 810 nm laser pulses is related to the following reasons, all of which point to a stronger ensemble interaction of the particles with green light compared with excitation at the LP (810 nm) wavelength:

- All particles in a typical lot of AuNRs interact with green light through the TP peak of the nanorods, but also through the several percent nanospheres which are unavoidably present as byproduct (Figure 2, Supporting Information). A typical sample of AuNRs is not monodisperse, this means that with monochromatic laser irradiation in the region of the LP peak, only a fraction of the AuNRs will interact with the light.
- Excitation at either LP or TP peaks causes rapid heating of AuNRs and leads to their restructuring into shorter AuNRs and AuNSs. In the case of LP peak excitation, after the shape transformation during the first pulse(s), there are less or no AuNRs left to absorb at the LP wavelength during subsequent pulses. On the other hand, when AuNR reshaping into spheres takes place under the influence of 532 nm pulses, progressively more particles can interact with green light due to the plasmon peak at around 520 nm.
- Heat production/dissipation or bubble formation/cavitation, the initiators of cell damage are thus more likely to take place when 532 nm pulses are used compared to LP excitation if fluences above the reshaping threshold are used.
- Interaction of mAb-AuNR with receptors on the target cell surface is followed by incorporation of the particles in vesicles. The AuNRs could undergo plasmonic coupling[49,50] with each other or undergo aggregation resulting in considerable changes in the optical properties by shifting of the LP peaks due to plasmon coupling effects.

The mechanism of cell death is most likely due to bubble formation and collapse rather than due to thermal stresses. The thermal mechanism of cell death has been shown to require fluences of laser energy in the range[22] 30 to 1000 J $cm^{-2}$. On the other hand, the bubble mechanism requires lower fluences of the order of 1 J $cm^{-2}$ when mediated by single gold particles. The threshold for bubble formation is lower for clusters of nanoparticles[30,45,46,56] than for individual particles due to reduced surface tension and larger optical absorption cross-section. The reduced threshold energy will also lead to larger bubbles.[57] Considering that cell death in our case occurs at around 60 mJ $cm^{-2}$ it is very likely that bubble formation from multiple particles occurs. The bubble sizes depend upon the sizes of the clusters involved, but can be as large as the cell.[30] In such a case, rupture of the plasma membrane of the cell can cause necrosis and lysis in the cell. Although the devastating effect of larger bubbles in living tissue have been studied extensively and, e.g., related to tissue dilation and invagination[58] or to liquid jet formation,[59] the precise mechanism of cell death by bubbles is still subject of research. Recently, these effects, including the unexpected influence of the mechanical properties of the tissue surroundings, have also been observed for much smaller bubbles.[60]

The control SKBR3 cells (no incubation with nanoparticles) irradiated at 810 and 532 nm were not affected, and they are shown in the Supporting Information.

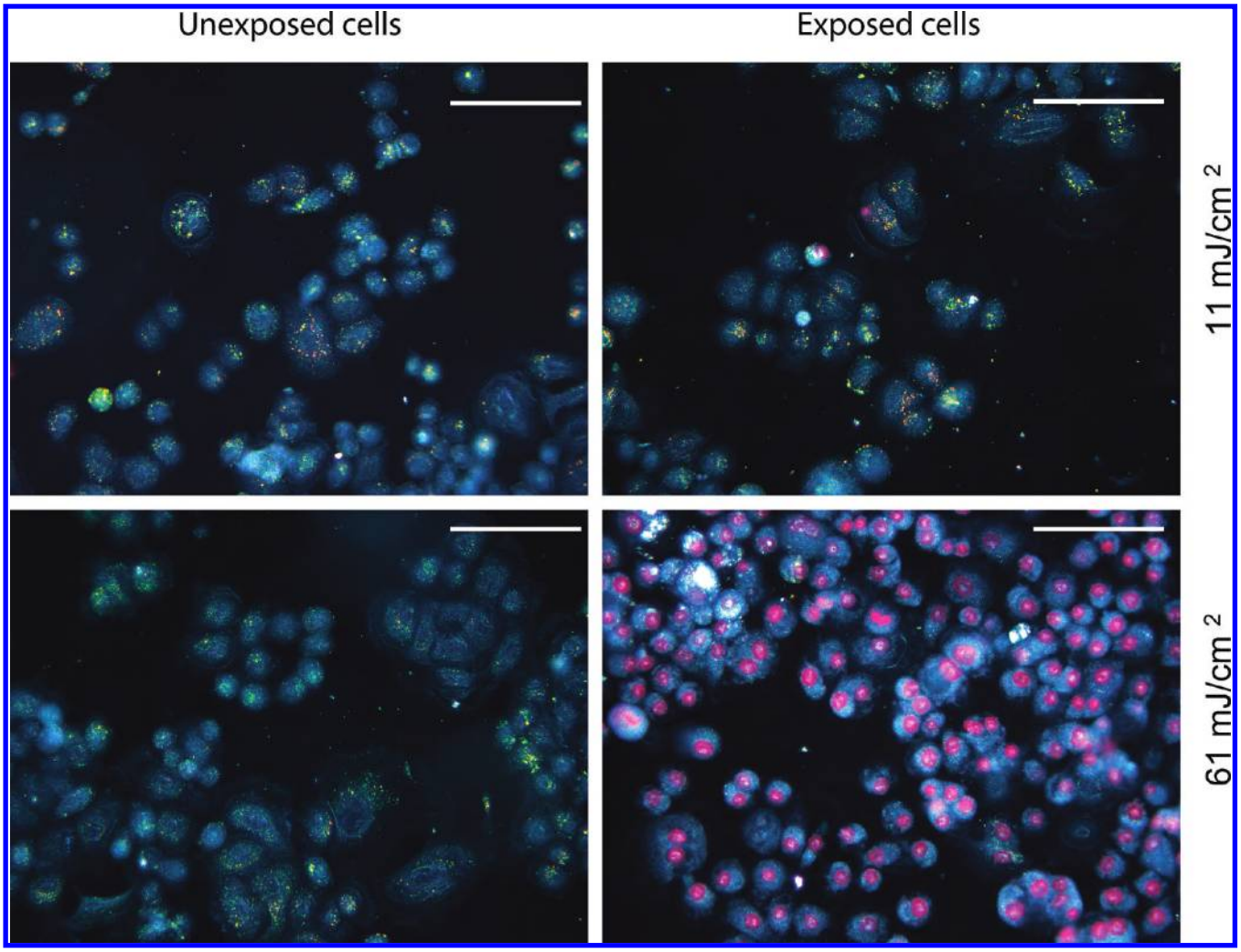


**Figure 8.** Dark-field light scattering microscopic images (scale bar 50 $\mu$m) of SKBR3 cells incubated with mAb-AuNR$_{810}$ for 24 h. Left column for nonirradiated cells and right column for cells irradiated at 532 nm with fluences of 11 and 61 mJ cm$^{-2}$ per pulse. For the fluence of 11 mJ cm$^{-2}$ the cells are alive as seen by the PI exclusion, but for 61 mJ cm$^{-2}$ cells take up PI showing that extensive cell death has occurred.

**Concluding Remarks.** A spectroscopic study of AuNR samples illuminated with various nanosecond laser fluences at the LP peak, allowed us to ascertain a threshold value ($F_{th}$) at which 50% of the population has undergone photothermal reshaping to lower aspect ratio NRs and spheres.

We used dark-field light-scattering color changes to identify the shape transformations, when SKBR3 cells incubated with mAb-AuNR, were irradiated with various fluences at the LP peak of the particles. An important finding was that while reshaping did take place at the fluences used, no direct lethal damage to cells was inflicted as monitored by propidium iodide exclusion. On the other hand, using irradiation at the TP peak wavelength, at comparative fluences, extensive cell death was achieved as seen in propidium iodide uptake. We surmise that presence of spheres as byproduct, the lower but ubiquitous TP, the photoreshaping of AuNR into spheres, and clustering of AuNR inside cells provides a sufficiently high optical absorption at 532 nm.

TEM imaging of cell sections incubated with mAb-AuNR showed the sequestering of large numbers of particles in vesicles. The mechanism of cell death with the use of TP peak irradiation was not investigated, but is thought to be due to bubble formation from these NR clusters. This appears to be the only plausible explanation for achieving cell death with moderately low fluences.

An important issue that needs to be considered is based on the TEM findings supporting the possibility of plasmonic interactions of NRs in clusters in the cell. This provokes the question: is it then necessary to engineer plasmonic nanoparticles in the laboratory with the ideal location of the absorption peak in the NIR window, only to have this characteristic peak 'corrupted' by interaction with cells? From the in vivo application point of view, green light can still be used for treating superficial tumors with topical application of the mAb-AuNRs. For deeper lying (10 mm+) tumors, green light delivery could be achieved with the use of optical fibers[61] guided using ultrasound imaging, in combination with systemic administration of the mAb-AuNRs.

## ■ ASSOCIATED CONTENT

**Supporting Information.** Additional experimental details including figures. This material is available free of charge via the Internet at http://pubs.acs.org.

## AUTHOR INFORMATION

**Corresponding Author**
*E-mail: c.ungureanu@tue.nl; s.manohar@utwente.nl.

## ACKNOWLEDGMENT

This work is funded through the thrust area program NIMTIK of the University of Twente; through the PRESMITT project (IPD067771) of the SenterNovem program IOP Photonic Devices; and by the Nederlandse Wetenschappelijk Organisatie (NWO) and Stichting Technische Wetenschappen (STW) through project TTF 6527; and by a KWF-translational research award (Grant No. PGF 2009-4344; FvL)

## REFERENCES

(1) Perez-Juste, J.; Pastoriza-Santos, I.; Liz-Marzan, L. M.; Mulvaney, P. *Coord. Chem. Rev.* **2005**, *249*, 1870–1901.36th International Conference on Coordination Chemistry, Merida, Mexico, July 2004.
(2) Huang, X.; Neretina, S.; El-Sayed, M. A. *Adv. Mater.* **2009**, *21*, 4880–4910.
(3) Nikoobakht, B.; El-Sayed, M. A. *Chem. Mater.* **2003**, *15*, 1957–1962.
(4) Rayavarapu, R. G.; Petersen, W.; Ungureanu, C.; Post, J.; van Leeuwen, T. G.; Manohar, S. *Int. J. Biomed. Imaging* **2007**, *2007*, 29817.
(5) Cheong, S.-K.; Krishnan, S.; Cho, S. *Med. Phys.* **2008**, *35*, 2708–2708.
(6) Wang, L. V. *Nat. Photonics* **2009**, *3*, 503–509.
(7) Piras, D.; Xia, W.; Steenbergen, W.; van Leeuwen, T.; Manohar, S. *IEEE J. Selected Top. Quantum Electron.* **2010**, *16*, 730–739.
(8) Ermilov, S.; Khamapirad, T.; Conjusteau, A.; Leonard, M.; Lacewell, R.; Mehta, K.; Miller, T.; Oraevsky, A. J. *Biomed. Opt* **2009**, *14*, 024007.
(9) Oraevsky, A. A.; Karabutov, A. A.; Savateeva, E. V. *Proc. SPIE* **2001**, *4434*, 60–69.
(10) Tong, L.; Wei, Q.; Wei, A.; Cheng, J.-X. *Photochem. Photobiol.* **2009**, *85* (12), 21–32.
(11) Agarwal, A.; Huang, S. W.; OŠDonnell, M.; Day, K. C.; Day, M.; Kotov, N.; Ashkenazi, S. J. *Appl. Phys* **2007**, *102*, 064701–4.
(12) Eghtedari, M.; Liopo, A. V.; Copland, J. A.; Oraevsky, A. A.; Motamedi, M. *Nano Lett.* **2009**, *9*, 287–291.
(13) Li, C.; Wang, L. V. *Phys. Med. Biol.* **2009**, *54*, R59–R97.
(14) Pissuwan, D.; Valenzuela, S. M.; Cortie, M. B. *Biotechnol. Genet. Eng. Rev.* **2008**, *25*, 93–112.
(15) Day, E. S.; Morton, J. G.; West, J. L. *J. Biomech. Eng.* **2009**, *131*, 074001.
(16) Li, J.-L.; Gu, M. *IEEE J. Quantum Electron.* **2009**, (*99*), PP1−8.
(17) Liu, C.; Li, Z.; Zhang, Z. J *Biol. Phys.* **2009**, *35*, 175–183.
(18) von Maltzahn, G.; Park, J.-H.; Agrawal, A.; Bandaru, N. K.; Das, S. K.; Sailor, M. J.; Bhatia, S. N. *Cancer Res.* **2009**, *69* (9), 3892–3900.
(19) Niidome; Takuro; Akiyama; Yasuyuki; Yamagata; Masato, K.; Takahito, T. N.; Mori; Yasuro, K.; Yoshiki *J. Biomater. Sci. Polym. Ed.* **2009**, *20* (13), 1203–1215.
(20) Yang, X.; Stein, E. W.; Ashkenazi, S.; Wang, L. V. *WIREs Nanomed. Nanobiotechnol.* **2009**, *1*, 360–368.
(21) Cole, J. R.; Mirin, N. A.; Knight, M. W.; Goodrich, G. P.; Halas, N. J. *J. Phys. Chem. C* **2009**, *113* (28), 12090–12094.
(22) Lukianova-Hleb, E. Y.; Hanna, E.; Hafner, J. H.; Lapotko, D. O. *Nanotechnology* **2010**, *21* (8), 085102–8.
(23) Grobmyer, S. R., Moudgil, B. M., Eds. *Cancer Nanotechnology*; Humana Press, 2010.
(24) Didychuk, C. L.; Ephrat, P.; Chamson-Reig, A.; Jacques, S. L.; Carson, J. J. L. *Nanotechnol* **2009**, *20*, 195102–195111.
(25) Kim, J.-W.; Galanzha, E. I.; Shashkov, E. V.; Moon, H.-M.; Zharov, V. P. *Nature Nanotechnol.* **2009**, *4*, 688–694.
(26) Tong, L.; Zhao, Y.; Huff, T. B.; Hansen, M. N.; Wei, A.; Cheng, J.-X. *Adv. Mater.* **2007**, *19*, 3136–3141.
(27) Li, J.-L.; Gu, M. *Biomaterials* **2010**, *31*, 9492–9498.
(28) Huff, T. B.; Tong, L.; Zhao, Y.; Hansen, M. N.; Cheng, J.-X.; Wei, A. *Nanomedicine* **2007**, *2* (1), 125–132.
(29) Day, E. S.; Bickford, L. R.; Slater, J. H.; Riggall, N. S.; Drezek, R. A.; West, J. L. *Int. J. Nanomed.* **2010**, *5*, 445–454.
(30) Lapotko, D.; Lukianova, E.; Potapnev, M.; Aleinikova, O.; Oraevsky, A. *Cancer Lett.* **2006**, *239*, 36–45.
(31) Takahashi1, H.; Niidome, T.; Nariai, A.; Niidome, Y.; Yamada, S. *Chem. Lett.* **2006**, *35* (5), 500–501.
(32) Takahashi, H.; Niidome, T.; Nariai, A.; Niidome, Y.; Yamada, S. *Nanotechnology* **2006**, *17*, 4431–4435.
(33) Chang, S.-S.; Shih, C.-W.; Chen, C.-D.; Lai, W.-C.; Wang, C. R. C. *Langmuir* **1999**, *15*, 701–709.
(34) Link, S.; Wang, Z. L.; El-Sayed, M. A. *J. Phys. Chem. B* **2000**, *104* (33), 7867–7870.
(35) Link, S.; El-Sayed, M. A. *J. Phys. Chem. B* **1999**, *103*, 4212–4217.
(36) Link, S.; El-Sayed, M. A. *J. Chem. Phys.* **2000**, *114*, 2362–2368.
(37) Link, S.; Burda, C.; Nikoobakht, B.; El-Sayed, M. A. *J. Phys. Chem. B* **2000**, *104* (26), 6152–6163.
(38) Link, S.; Burda, C.; Mohamed, M. B.; Nikoobakht, B.; El-Sayed, M. A. *J. Phys. Chem. A* **1999**, *103* (9), 1165–1170.
(39) Chen, L.-C.; Wei, C.-W.; Souris, J. S.; Cheng, S.-H.; Chen, C.-T.; Yang, C.-S.; Li, P.-C.; Lo, L.-W. *J. Biomed. Opt* **2010**, *15*, 016010.
(40) Wei, C.-W.; Huang, S.-W.; Wang, C.-R. C.; Li, P.-C. *IEEE Trans. Ultrason. Ferroelectr. Freq. Control* **2007**, *54* (6), 1131–41.
(41) Chen, Y. S.; Frey, W.; Kim, S.; Homan, K.; Kruizinga, P.; Sokolov, K.; Emelianov, S. *Opt. Express* **2010**, *18*, 8867–8878.
(42) Rayavarapu, R. G.; Petersen, W.; Chin, P.; Janssen, H.; van Leeuwen, F. W. B.; Manohar, S.; van Leeuwen, T. G. *Nanotechnology* **2010**, *21*, 145101.
(43) Lapotko, D. O.; Lukianova-Hleb, E. Y.; Oraevsky, A. A. *Nanomedicine* **2007**, *2*, 241–53.
(44) Ratto, F.; Matteini, P.; Centi, S.; Rossi, F.; Pini, R. J *Biophoton* **2010**, DOI 10.1002, 1−10.
(45) Khlebtsov, B.; Zharov, V.; Melnikov, A.; Tuchin, V.; Khlebtsov, N. *Nanotechnology* **2006**, *17*, 5167–5179.
(46) Wagner, D. S.; Delka, N. A.; Lukianova-Hleb, E. Y.; Hafner, J. H.; Farach-Carson, M. C.; Lapotko, D. O. *Biomaterials* **2010**, *31* (29), 7567–7574.
(47) Lukianova-Hleb, E. Y.; Santiago, C.; Wagner, D. S.; Hafner, J. H.; Lapotko, D. O. *Nanotechnology* **2010**, *21*, 225102.
(48) Ungureanu, C.; Rayavarapu, R. G.; Manohar, S.; van Leeuwen, T. G. *J. Appl. Phys.* **2009**, *105*, 102032.
(49) Jain, P. K.; Eustis, S.; El-Sayed, M. A. *J. Phys. Chem. B* **2006**, *110* (37), 18243–18253.
(50) Funston, A. M.; Novo, C.; Davis, T. J.; Mulvaney, P. *Nano Lett.* **2009**, *9* (4), 1651–1658.
(51) Horiguchi, Y.; Honda, K.; Kato, Y.; Nakashima, N.; Niidome, Y. *Langmuir* **2008**, *24* (20), 12026–12031.
(52) Link, S.; Burda, C.; Nikoobakht, B.; El-Sayed, M. *Chem. Phys. Lett.* **1999**, *315*, 12–18.
(53) Plech, A.; Cerna, R.; Kotaidis, V.; Hudert, F.; Bartels, A.; Dekorsy, T. *Nano Lett* **2007**, *7*, 1026–1031.
(54) Lukianova-Hleb, E. Y.; Anderson, L. J. E.; Lee, S.; Hafner, J. H.; Lapotko, D. O. *Phys. Chem. Chem. Phys.* **2010**, *12*, 12237–12244.
(55) Wang, Y.; Teitel, S.; Dellago, C. *Nano Lett.* **2005**, *5* (11), 2174–2178.
(56) Kitz, M.; Preisser, S.; Wetterwald, A.; Jaeger, M.; Thalmann, G. N.; Frenz, M. *Biomed. Opt. Express.* **2011**, *2*, 291–304.
(57) van Leeuwen, T. G.; Jansen, E. D.; Welch, A. J.; Borst, C. *Lasers Surg. Med.* **1996**, *18* (4), 381–190.
(58) van Leeuwen, T. G.; Meertens, J.; Velema, E.; Post, M.; Borst, C. *Circulation* **1993**, *87* (4), 1258–63.
(59) Vogel, A.; Venugopalan, V. *Chem. Rev.* **2003**, *103*, 577–644.
(60) Chen, H.; Kreider, W.; Brayman, A. A.; Bailey, M. R.; Matula, T. J. *Phys. Rev. Lett.* **2011**, *106*, 034301.
(61) Lukianova-Hleb, E. Y.; Oginsky, A. O.; Samaniego, A. P.; Shenefelt, D. L.; Wagner, D. S.; Hafner, J. H.; Farach-Carson, M. C.; Lapotko, D. O. *Theranostics* **2011**, *1*, 3–17.